CORE
Metadata, citation and similar papers at core.ac.uk
Provided by VCU Scholars Compass

Virginia Commonwealth University
VCU Scholars Compass

Electrical and Computer Engineering Publications
Dept. of Electrical and Computer Engineering

2008

Cavity polaritons in ZnO-based hybrid microcavities

R. Shimada
Virginia Commonwealth University, rshimada@vcu.edu

J. Xie
Virginia Commonwealth University

Vitaliy Avrutin
Virginia Commonwealth University, vavrutin@vcu.edu

Ü. Özgür
Virginia Commonwealth University, uozgur@vcu.edu

Hadis Morkoç
Virginia Commonwealth University, hmorkoc@vcu.edu

Follow this and additional works at: http://scholarscompass.vcu.edu/egre_pubs


Part of the Electrical and Computer Engineering Commons

Shimada, R., Xie, J., Avrutin, V., et al. Cavity polaritons in ZnO-based hybrid microcavities. Applied Physics Letters, 92, 011127 (2008). Copyright © 2008 AIP Publishing LLC.

Downloaded from
http://scholarscompass.vcu.edu/egre_pubs/92

This Article is brought to you for free and open access by the Dept. of Electrical and Computer Engineering at VCU Scholars Compass. It has been accepted for inclusion in Electrical and Computer Engineering Publications by an authorized administrator of VCU Scholars Compass. For more information, please contact libcompass@vcu.edu.

Cavity polaritons in ZnO-based hybrid microcavities

R. Shimada,[a] J. Xie, V. Avrutin, Ü. Özgür, and H. Morkoč
Department of Electrical and Computer Engineering, School of Engineering, Virginia Commonwealth University, Richmond, Virginia 23284, USA

(Received 15 October 2007; accepted 7 December 2007; published online 10 January 2008)

Among wide-bandgap semiconductors, ZnO is a very attractive candidate for blue-ultraviolet lasers operating at room temperature owing to its large exciton binding energy and oscillator strength. Especially, ZnO-based microcavity structures are most conducive for polariton lasing at room temperature. We report the observation of cavity polaritons in bulk ZnO-based hybrid microcavities at room temperature. The bulk ZnO-based hybrid microcavities are composed of 29 pairs of $Al_{0.5}Ga_{0.5}N/GaN$ distributed Bragg reflector (DBR) at the bottom of the λ-thick cavity layer and eight pairs of SiO_2/Si_3N_4 DBR as the top mirror, which provided cavity Q values of ~100. Anticrossing behavior between the lower and upper polariton branches was observed at room temperature. From the polariton dispersion curve, the vacuum Rabi splitting was estimated to be ~50 meV. These results are promising toward the realization of ZnO-based microcavity polariton devices. © *2008 American Institute of Physics*. [DOI: 10.1063/1.2830022]

Since the first report of the coupled exciton-photon mode splitting in GaAs-based microcavities (MCs),[1] planar semiconductor MCs attracted a great deal of attention due to the possibilities of enhancement and control of the interaction between photons and excitons in these structures. The coupled exciton-photon mode, namely, cavity polaritons,[2] which are the elementary optical excitations in semiconductor MCs, may be viewed as a superposition of excitons and cavity photons. The major feature of the cavity polariton technology centers around large and unique optical nonlinearities, which would lead to another class of optical devices such as polariton lasers having very low thresholds[3,4] and polariton parametric amplifiers with ultrafast response.[5,6] From the point of view of materials, the experimental observations of these features at room temperature (RT) are prevented in GaAs-based MCs because of the slow relaxation of photoexcited polaritons down to the bottom of the lower polariton branch. In II-VI semiconductors, the large exciton binding energy allows the observation of nonlinearities up to 220 K in CdTe-based MCs,[6] however, the II-VI technology has not yet been proven technologically so far. On the other hand, III-nitride based semiconductors are much likely to exhibit cavity polaritons at RT and make polariton based devices possible due to the large exciton binding energy [~26 meV for bulk GaN layers and >40 meV in narrow quantum wells (QWs)] and strong coupling to the light field. Several groups have already reported polariton luminescence at RT from bulk[7,8] and QW (Ref. 9) GaN-based MCs. Recently, polariton lasing at RT in bulk GaN-based MCs in the strong coupling regime was observed under the nonresonant pulsed optical pumping.[10] Another wide-bandgap semiconductor, ZnO is even a more attractive candidate for polariton lasers at RT owing to ~60 meV bulk exciton binding energy, which is almost twice larger than that of GaN. Zamfirescu *et al.*[11] predicted a large vacuum Rabi splitting, Ω_{Rabi} ~120 meV, for cavity polaritons in an all-ZnO-based MC that contains two $Mg_{0.3}Zn_{0.7}O/ZnO$ distributed Bragg reflectors (DBRs), which projects to an extremely low threshold polariton laser (~2 mW) at RT. A record Ω_{Rabi} of ~191 meV has been predicted in a model one-wavelength (λ)-thick ZnO-based MC utilizing SiO_2/ZrO_2 bottom and top DBRs.[12] However, there have been no experimental verifications of these values and even no reports on observation of cavity polaritons in ZnO-based MCs.

In this letter, we report the growth and characterization of bulk ZnO-based hybrid MCs, which exhibit strong coupling between the exciton and cavity modes. The investigated structure consists of a λ-thick bulk ZnO cavity layer sandwiched between a 29 pair $Al_{0.5}Ga_{0.5}N/GaN$ DBR and an 8 pair SiO_2/Si_3N_4 DBR used for bottom and top reflectors, respectively. The anticrossing behavior was observed in angle-resolved photoluminescence (PL) measurements at RT.

The bottom DBR was directly grown on a 200-nm-thick AlN buffer layer on (0001) sapphire substrate by low-pressure metal-organic chemical vapor deposition. The AlN buffer is chosen to avoid cracking due to the built-in strain caused by the lattice mismatch. Trimethylgallium (TMGa), trimethylaluminum (TMAl), and ammonia (NH_3) were used as sources for Ga, Al, and N, respectively. After depositing a 200-nm-thick AlN layer at 1050 °C, the wafer temperature was ramped to 1000 °C for the 29 pair AlGaN/GaN DBR growth. The V/III ratio was set to 2000 with a ~300 nm growth rate for AlGaN and GaN to achieve smooth interfaces. The Al composition in the DBR was nearly 50% as confirmed by high-resolution x-ray diffraction. A λ-thick (~160 nm considering $\lambda \approx 380$ nm in air) ZnO cavity layer was grown at the bottom AlGaN/GaN DBR by plasma-assisted molecular beam epitaxy (MBE) in a manner similar to that of ZnO grown on epitaxial-GaN.[13] The bottom DBR was heat treated in the MBE system for ~15 min below 700 °C and then exposed to a Zn beam before the ZnO growth for preventing oxidation of the Al(Ga)N layer. The ZnO growth was carried out at 650 °C following the deposition of a low temperature ZnO buffer layer at 300 °C under oxygen rich conditions. The growth mode was two dimensional as monitored *in situ* by reflection high energy electron diffraction. PL spectrum at RT shows the suppression of the deep level emission band of ZnO in Fig. 1(a), which indi-

[a]Electronic mail: rshimada@vcu.edu.

This article is copyrighted as indicated in the article. Reuse of AIP content is subject to the terms at: http://scitation.aip.org/termsconditions. Downloaded to IP: 128.172.48.59 On: Wed, 08 Apr 2015 16:50:26

 © 2008 American Institute of Physics

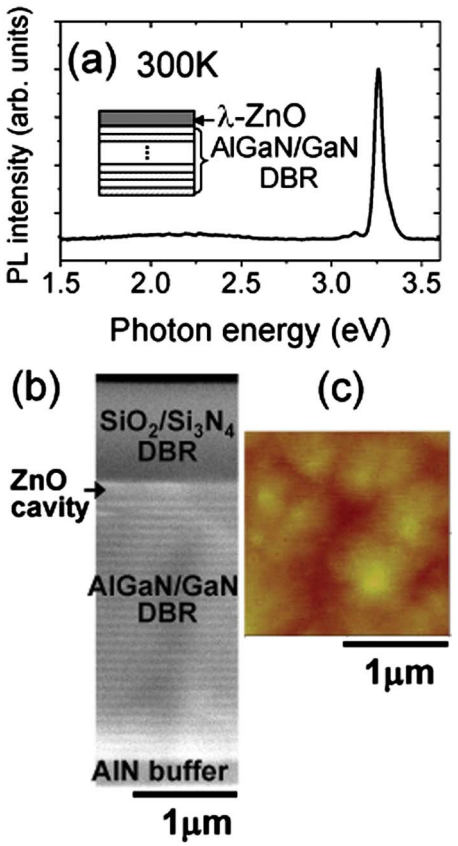

FIG. 1. (Color online) (a) Room temperature (RT) photoluminescence (PL) spectrum from a half cavity (without the top DBR). The inset shows the sample structure. (b) Cross-sectional SEM image of a λ-thick ZnO-based hybrid microcavity (MC). (c) AFM image of the ZnO cavity layer grown on the bottom DBR. rms surface roughness is 1.3 nm over an area of 2×2 μm^2.

cates good material quality. To complete the MC structure an eight pair SiO_2/Si_3N_4 dielectric DBR was deposited by ultrahigh vacuum remote plasma enhanced chemical vapor deposition on ZnO. As seen from the cross sectional scanning electron microscope (SEM) image of the ZnO hybrid MC in Fig. 1(b), the interface between the bottom DBR and the ZnO cavity layer is fairly smooth, though the SiO_2/Si_3N_4 DBR interface is not very clear. The rms surface roughness of the ZnO cavity layer, determined from the atomic force microscopy (AFM) image shown in Fig. 1(c), was 1.3 nm over a 2×2 μm^2 area, while the bottom DBR surface had a rms roughness of 1.0 nm over the same area and exhibited atomic steps.

A typical reflectivity spectrum at RT (solid line) from a 29 pair $Al_{0.5}Ga_{0.5}N/GaN$ DBR for near-normal incidence and the spectrum calculated using the transfer matrix method[14] (dashed line) are shown in Fig. 2(a). The refractive index values used for the calculation were taken from Brunner *et al.*[15] The measured peak reflectivity and the stop bandwidth are ~90% and ~150 meV, respectively, for the 29 pair $Al_{0.5}Ga_{0.5}N/GaN$ DBR, both smaller than the calculated values. This discrepancy is due to the likely variations of the thickness and variations in the Al composition as the sample was not rotated during growth. The PL spectrum from a half-MC (without the top SiO_2/Si_3N_4 DBR) at 300 K is also shown in Fig. 2(a). The PL emission peak from the ZnO cavity layer (3.29 eV) was located within the stop band in the bottom DBR, which is imperative. Figure 2(b) shows the

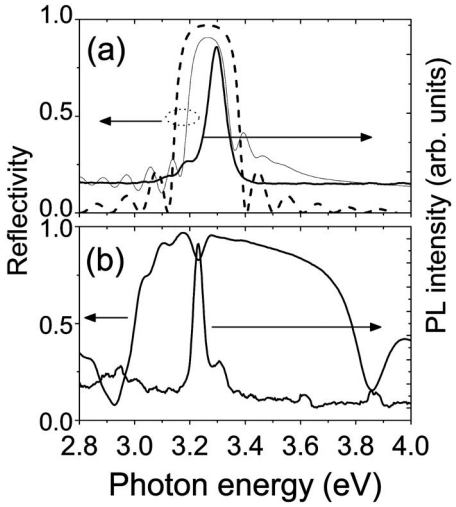

FIG. 2. (a) RT reflectivity spectrum of a 29 pair $Al_{0.5}Ga_{0.5}N/GaN$ DBR (thin solid line) showing a peak reflectivity of ~90% and a stop bandwidth of ~150 meV. The dashed line shows the calculated reflectivity spectrum using the transfer matrix method. RT PL spectrum (thick solid line) from a half cavity (without top SiO_2/Si_3N_4 DBR) shows that the peak position is located within the stopband of the bottom DBR. (b) RT reflectivity and PL spectra from the full MC. The PL peak and the dip in reflectivity are in good agreement.

reflectivity and PL spectra from the full-MC (including the top SiO_2/Si_3N_4 DBR) at near-normal incidence. The energy of the observed reflectivity dip is consistent with the PL emission peak from a full-MC (3.23 eV), which corresponds to the lower polariton mode from the ZnO-based hybrid MC. A cavity quality value (Q value) of ~100 was obtained from both the reflectivity and PL spectra. A weak emission peak at 3.30 eV, which corresponds to the upper polariton mode, was also observed. However, the observation of the upper and lower polariton modes is strongly dependent on sample position, due to the thickness nonuniformity in the ZnO cavity layer and the bottom DBR.

Angle-resolved measurements can be used to trace the polariton modes in MCs without any change in the position or temperature. Angle-resolved PL measurements were conducted at RT under a weak excitation power density using a He–Cd laser. The laser beam was focused on the sample surface and the PL was collected by a 400 μm core optical fiber at different angles. The PL spectra at RT were measured from 0° to 40°, as shown in Fig. 3(a). For reference, the PL spectrum from a half-MC (dashed line) is also shown in the upper part of the figure. It is clear that the lower polariton mode gets close to the uncoupled exciton mode, and the upper polariton mode is dispersed from the exciton mode to the cavity mode. The experimental cavity polariton dispersion curve shown in Fig. 3(b) exhibits a typical anticrossing behavior between the cavity mode and exciton mode when the cavity mode energy crosses the exciton mode. Although the resolution of the upper polariton branch was limited in the angle-resolved PL spectra, the anticrossing behavior confirms the strong coupling regime in hybrid ZnO-based MCs. A vacuum Rabi splitting of ~50 meV is estimated at the resonant condition of $\theta=22°$, which is larger than that reported in bulk-GaN hybrid MCs,[7] but smaller than that predicted by Zamfirescu *et al.*[11] We believe that the shortcoming is due to the inhomogeneous broadening in the ZnO cavity layer. Since the stop bandwidth of the bottom DBR is narrow (~150 meV) due to relatively low refractive index contrast

This article is copyrighted as indicated in the article. Reuse of AIP content is subject to the terms at: http://scitation.aip.org/termsconditions. Downloaded to IP: 128.172.48.59 On: Wed, 08 Apr 2015 16:50:26

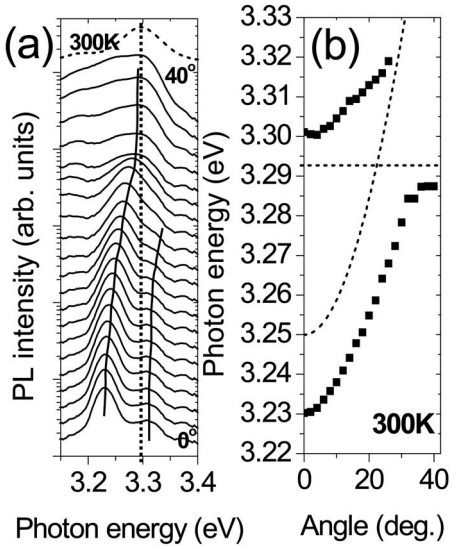

FIG. 3. (a) Angle-resolved PL spectra at RT in the range of 0°–40° for a λ-thick ZnO hybrid MC. The dotted line is the exciton mode. The solid lines are guides to the eye. (b) Experimental cavity polariton dispersion curve. The dashed lines represent the cavity and exciton modes.

in semiconductor layers and, therefore, the upper polariton features are not clear at large angles, it might be difficult to observe a clear anticrossing behavior. However, it should be noted that polariton lasing depends on the formation of a Bose-Einstein condensate in the lower energy trap states defined by the lower polariton branch. Therefore, clear observation of the lower polariton branch with a large Rabi splitting is the basic requirement for realization of the polariton laser, and clear tracing of the upper polariton branch, especially at large angles, is not absolutely necessary to prove the existence of a strong coupling regime. Under the weak excitation conditions employed in our study, the nonlinear features indicative of lasing cannot be observed in the PL spectra at RT. In addition, higher Q-value MCs are required for nonlinear effects in MCs.

In summary, cavity polaritons in a ZnO-based hybrid MC, which is sandwiched between a 29 pair $Al_{0.5}Ga_{0.5}N/GaN$ DBR and an 8 pair SiO_2/Si_3N_4 DBR, have been observed, paving the way for polariton lasers operating at RT. In angle-resolved PL measurements at RT, the anticrossing behavior between the cavity and exciton modes was evident. A large vacuum Rabi splitting of ~50 meV at RT was obtained from the cavity polariton dispersion curve, which is larger than that observed in bulk GaN-based MCs. Our results indicate that ZnO-based microcavities can be used to realize polariton lasers.

This work was supported by Air Force Office Scientific Research under the direction of Dr. K. Reinhardt and D. D. Silversmith.

[1] C. Weisbush, M. Nishioka, A. Ishikawa, and Y. Arakawa, Phys. Rev. Lett. **69**, 3314 (1992).
[2] For a review see, e.g., M. S. Skolnick, T. A. Fisher, and D. M. Whittaker, Semicond. Sci. Technol. **13**, 645 (1998).
[3] A. Imamoğlu, R. J. Ram, S. Pau, and Y. Yamamoto, Phys. Rev. A **53**, 4250 (1996).
[4] G. Malpuech, A. Kavokin, A. Di Carlo, and J. J. Baumberg, Phys. Rev. B **65**, 153310 (2002).
[5] P. G. Savvidis, J. J. Baumberg, R. M. Stevenson, M. S. Skolnick, D. M. Whittaker, and J. S. Roberts, Phys. Rev. Lett. **84**, 1547 (2000).
[6] M. Saba, C. Ciuti, J. Bloch, V. Thierry-Mieg, R. Andre, L. Si Dang, S. Kundermann, A. Mura, G. Bongiovanni, J. L. Staehli, and B. Deveaud, Nature (London) **414**, 731 (2001).
[7] R. Butté, G. Christmann, E. Feltin, J.-F. Carlin, M. Mosca, M. Ilegems, and N. Grandjean, Phys. Rev. B **73**, 033315 (2006).
[8] A. Alyamani, D. Sanvitto, A. A. Khalifa, M. S. Skolnick, T. Wang, F. Ranalli, P. J. Parbrook, A. Tahraoui, and R. Airey, J. Appl. Phys. **101**, 093110 (2007).
[9] E. Feltin, G. Christmann, R. Butté, J.-F. Carlin, M. Mosca, and N. Grandjean, Appl. Phys. Lett. **89**, 071107 (2006).
[10] S. Christopoulos, G. Baldassarri Höger von Högersthal, A. J. D. Grundy, P. G. Lagoudakis, A. V. Kavokin, J. J. Baumberg, G. Christmann, R. Butté, E. Feltin, J.-F. Carlin, and N. Grandjean, Phys. Rev. Lett. **98**, 126405 (2007).
[11] M. Zamfirescu, A. Kavokin, B. Gil, G. Malpuech, and M. Kaliteevski, Phys. Rev. B **65**, 161205 (2002).
[12] S. F. Chichibu, A. Uedono, A. Tsukazaki, T. Onuma, M. Zamfirescu, A. Ohtomo, A. Kavokin, G. Cantwell, C. W. Litton, T. Sota, and M. Kawasaki, Semicond. Sci. Technol. **20**, S67 (2005).
[13] H. J. Ko, Y. Chen, S. K. Hong, and T. Yao, J. Cryst. Growth **209**, 816 (2000).
[14] M. Born and E. Wolf, *Principles of Optics*, 7th edition (Cambridge University Press, Cambridge, United Kingdom, 1999), p. 54.
[15] D. Brunner, H. Angerer, E. Bustarret, F. Freudenberg, R. Höpler, R. Dimitrov, O. Ambacher, and M. Stutzmann, J. Appl. Phys. **82**, 5090 (1997).

This article is copyrighted as indicated in the article. Reuse of AIP content is subject to the terms at: http://scitation.aip.org/termsconditions. Downloaded to IP: 128.172.48.59 On: Wed, 08 Apr 2015 16:50:26